We are IntechOpen, the world's leading publisher of Open Access books
Built by scientists, for scientists

6,900
Open access books available

186,000
International authors and editors

200M
Downloads

Our authors are among the

154
Countries delivered to

TOP 1%
most cited scientists

12.2%
Contributors from top 500 universities

CLARIVATE ANALYTICS
BOOK CITATION INDEX
INDEXED

WEB OF SCIENCE™

Selection of our books indexed in the Book Citation Index
in Web of Science™ Core Collection (BKCI)

Interested in publishing with us?
Contact book.department@intechopen.com

Numbers displayed above are based on latest data collected.
For more information visit www.intechopen.com

SQUID Magnetometers, Josephson Junctions, Confinement and BCS Theory of Superconductivity

Navin Khaneja

Abstract

A *s*uperconducting *qu*antum *i*nterference *d*evice (SQUID) is the most sensitive magnetic flux sensor currently known. The SQUID can be seen as a flux to voltage converter, and it can generally be used to sense any quantity that can be transduced into a magnetic flux, such as electrical current, voltage, position, etc. The extreme sensitivity of the SQUID is utilized in many different fields of applications, including biomagnetism, materials science, metrology, astronomy and geophysics. The heart of a squid magnetometer is a tunnel junction between two superconductors called a Josephson junction. Understanding the work of these devices rests fundamentally on the BCS theory of superconductivity. In this chapter, we introduce the notion of local potential and confinement in superconductivity. We show how BCS ground state is formed from interaction of wave packets confined to these local potential wells. The starting point of the BCS theory of superconductivity is a phonon-mediated second-order term that describes scattering of electron pair at Fermi surface with momentum $k_i, -k_i$ and energy $2\hbar\omega_i$ to $k_j, -k_j$ with energy $2\hbar\omega_j$. The transition amplitude is $\mathcal{M} = -\frac{d^2\omega_d}{\left(\omega_i - \omega_j\right)^2 - \omega_d^2}$, where d is the phonon scattering rate and ω_d is the Debye frequency. However, in the presence of offset $\omega_i - \omega_j$, there is also a present transition between states $k_i, -k_i$ and $k_j, -k_i$ of sizable amplitude much larger than $\mathcal{M}$. How are we justified in neglecting this term and only retaining $\mathcal{M}$? In this chapter, we show all this is justified if we consider phonon-mediated transition between wave packets of finite width instead of electron waves. These wave packets are in their local potentials and interact with other wave packets in the same well to form a local BCS state we also call BCS molecule. Finally, we apply the formalism of superconductivity in finite size wave packets to high T_c in cuprates. The copper electrons in narrow d-band live as packets to minimize the repulsion energy. The phonon-mediated coupling between wave packets (of width Debye energy) is proportional to the number of k-states in a packet, which becomes large in narrow d-band (10 times s-band); hence, d-wave T_c is larger (10 times s-wave). At increased doping, packet size increases beyond the Debye energy, and phonon-mediated coupling develops a repulsive part, destroying superconductivity at large doping levels.

Keywords: local potentials, superconductivity, phonons, Josephson junctions, squids

1. Introduction

There is a very interesting phenomenon that takes place in solid-state physics when certain metals are cooled below critical temperature of order of few Kelvin. The resistance of these metals completely disappears and they become superconducting. How does this happen? One may guess that maybe at low temperatures there are no phonons. That is not true, as we have low frequency phonons present. Why do we then lose all resistivity? Electrons bind together to form a molecule by phonon-mediated interaction. The essence of this interaction is that electron can pull on the lattice which pulls on another electron. This phonon-mediated bond is not very strong for only few meV, but at low temperatures, this is good enough; we cannot break it with collisions with phonons which only carry $k_B T$ amount of energy which is small at low temperatures. Then, electrons do not travel alone; they travel in a bunch, as a big molecule; and you cannot scatter them with phonon collisions.

This phenomenon whereby many materials exhibit complete loss of electrical resistance when cooled below a characteristic critical temperature [1, 2] is called superconductivity. It was discovered in mercury by Dutch physicist Onnes in 1911. For decades, a fundamental understanding of this phenomenon eluded the many scientists who were working in the field. Then, in the 1950s and 1960s, a remarkably complete and satisfactory theoretical picture of the classic superconductors emerged in terms of the Bardeen-Cooper-Schrieffer (BCS) theory [3]. Before we talk about the BCS theory, let us introduce the notion of local potentials.

Shown in **Figure 1** is a bar of metal. How are electrons in this metal bar? Solid-state physics texts start by putting these electrons in a periodic potential [4–6]. But that is not the complete story.

Shown in **Figure 2** is a periodic array of metal ions. Periodic arrangement divides the region into cells (region bounded by dashed lines in **Figure 2**) such that the potential in the ith cell has the form
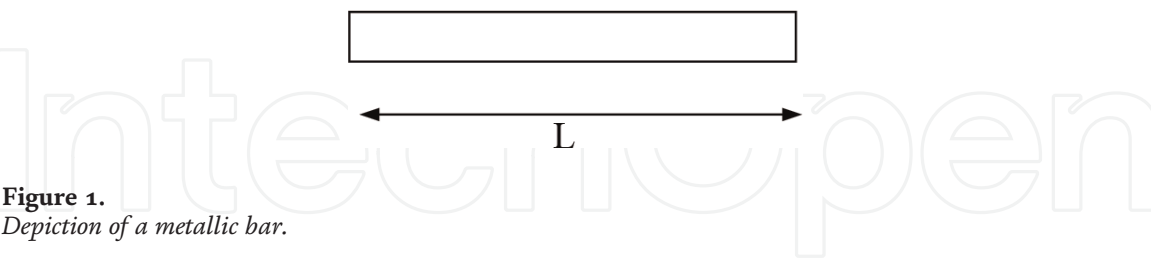

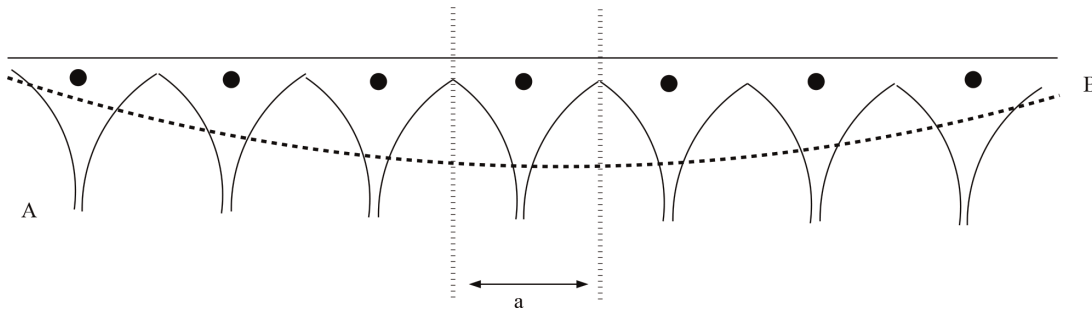**Figure 1.**
Depiction of a metallic bar.

Figure 2.
Depiction of the potential due to metal ions. A rapidly varying periodic part A *and slowly varying part* B.

$$V(x) = \underbrace{\frac{-Ze}{4\pi\epsilon_0}\frac{1}{|x-a_i|}}_{A} + \underbrace{\frac{-Ze}{4\pi\epsilon_0}\sum_{j\neq i}\frac{1}{|x-a_j|}}_{B},\tag{1}$$

where a_i is co-ordinate of the ion in the cell i. Eq. 1 has part A, the own ion potential. This gives the periodic part of the potential shown as thick curves in **Figure 2** and part B, the other ion potential. This is shown as dashed curve (trough or basin) in **Figure 2**. We do not talk much about this potential in solid-state physics texts though it is prominent (for infinite lattice, part B is constant that we can subtract). For $Z = 1$ and $a = 3A°$, we have $V_0 = \frac{e}{4\pi\epsilon_0 a} \sim 3V$. Then, the other ion potential has magnitude $\ln n\ V_0$ at its ends and $2\ln\frac{n}{2}\ V_0$ in the centre. The centre is deeper by $\sim \ln\frac{n}{2}V_0$. Let us say metal block is of length 30 cm with total sites $n = 10^9$; then, we are talking about a trough that is ~50 V deep. At room temperature, the kinetic energy of the electrons in $\frac{1}{2}k_BT = .02eV$ (as we will see subsequently, Fermi-Dirac statistics give much higher kinetic energies), the trough is deep enough to confine these electrons. It is this trough, basin or confining potential that we talk about in this chapter. Electrons move around in this potential as wave packets as shown in **Figure 3A**. Electrons can then be treated as a Fermi gas as shown in **Figure 3B**. While gas molecules in a container rebound of wall, the confining potential ensures electrons roll back before reaching the ends.

Coming back to a more realistic estimate of the kinetic energy, electron wave function is confined to length $L = na$ (due to confining potential); then, we can expand its eigenfunctions $\exp\left(i\frac{2\pi m}{na}x\right) = \exp(ikx)$ with energies $\frac{\hbar^2 k^2}{2m}$. We fill each k state with two electrons with $\frac{-\pi}{2a} \leq k \leq \frac{\pi}{2a}$, and kinetic energy of electrons goes from 0 to $\frac{\hbar^2\pi^2}{2a^2 m} \sim 5$ eV. This spread of kinetic energy is modified in the presence of periodic potential. We then have an energy band as shown in **Figure 4** with a bandwidth of 5–10 eV.

With this energy bandwidth, electrons are all well confined by the confining potential. In fact we do not need a potential of depth 50 eV; to confine the electrons, we can just do it with a depth of ~10 eV which means a length of around $L_0 \sim 300$ Å. It means electrons over length L_0 are confined, and due to *screening* by electrons outside L_0, they simply do not see any potential from ions outside this length. Thus, we get a local confining potential, and the picture is shown in **Figure 5**, many local wells. This is what we call *local potentials or local volumes*. Estimate of L_0 is a 1D calculation; in 3D it comes to a well of smaller diameter. However, if we account for *electron–electron repulsion*, then our earlier 1D estimate is probably okay. In any case, these numbers should be taken with a grain of salt. They are more qualitative than quantitative. The different wave packets in a local volume do not leave the volume as
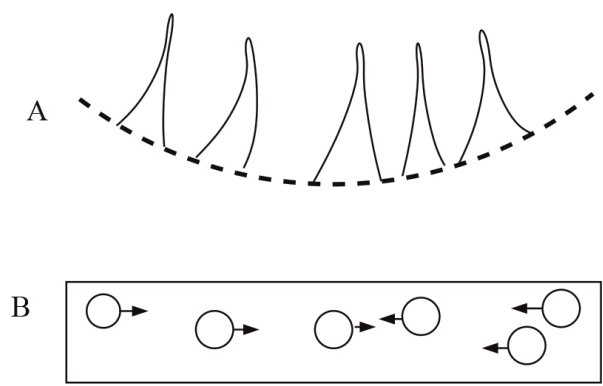

Figure 3.
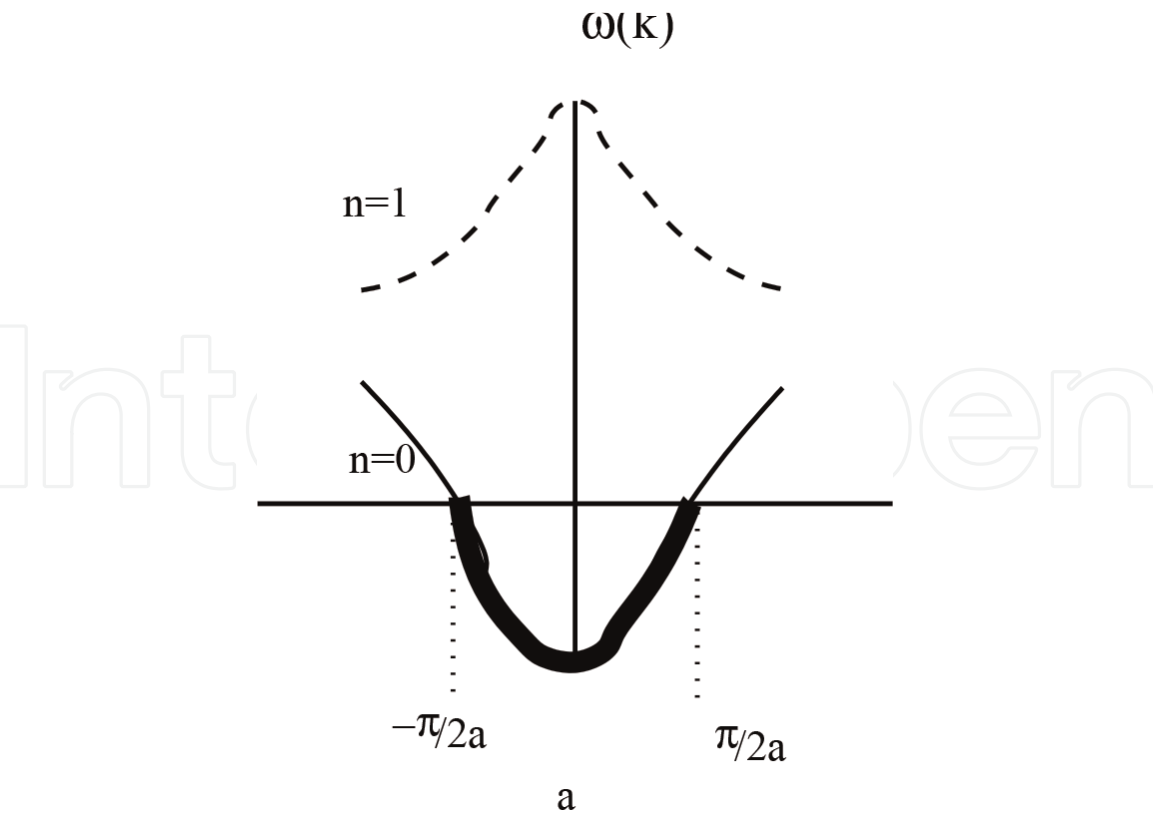*Depiction of Fermi gas of electrons in a metal moving in a confining potential.*

$$\omega(\kappa)$$

Figure 4.
The dispersion curve and energy band for electrons in a periodic potential.
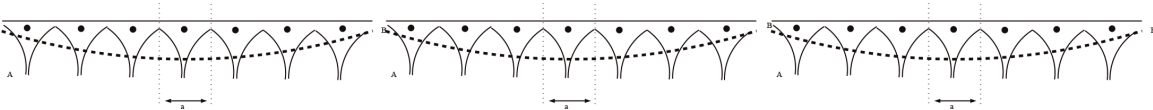

Figure 5.
Depiction of local potentials due to metal ions that locally confine electrons.

they see a local potential due to positive atomic ions. They just move back and forth in a local volume. When we apply an electric field say along x direction, the wave packets accelerate in that direction, and the local volume moves in that direction as a whole. This is electric current. Electrons are moving at very high velocity up to 10^5 m/s (Fermi velocity) in their local volumes, but that motion is just a back-and-forth motion and does not constitute current. The current arises when the local volume moves as a whole due to applied electric field. This is much slower at say drift velocity of 10^{-3} m/s for an ampere current through a wire of cross section 1 mm^2.

In this chapter, we spell out the main ideas of the BCS theory. The BCS theory tells us how to use phonon-mediated interaction to bind electrons together, so that we have big molecule and we call the BCS ground state or the BCS molecule. At low temperatures, phonons do not have energy to break the bonds in the molecule; hence, electrons in the molecule do not scatter phonons. So, let us see how BCS binds these electrons into something big.

2. Cooper pairs and binding

Let us take two electrons, both at the Fermi surface, one with momentum k_1 and other $-k_1$. Let us see how they interact with phonons. Electron k_1 pulls/plucks on the lattice due to Coulomb attraction and in the process creates (emits) a phonon and thereby recoils to new momentum k_2. The resulting lattice vibration is sensed
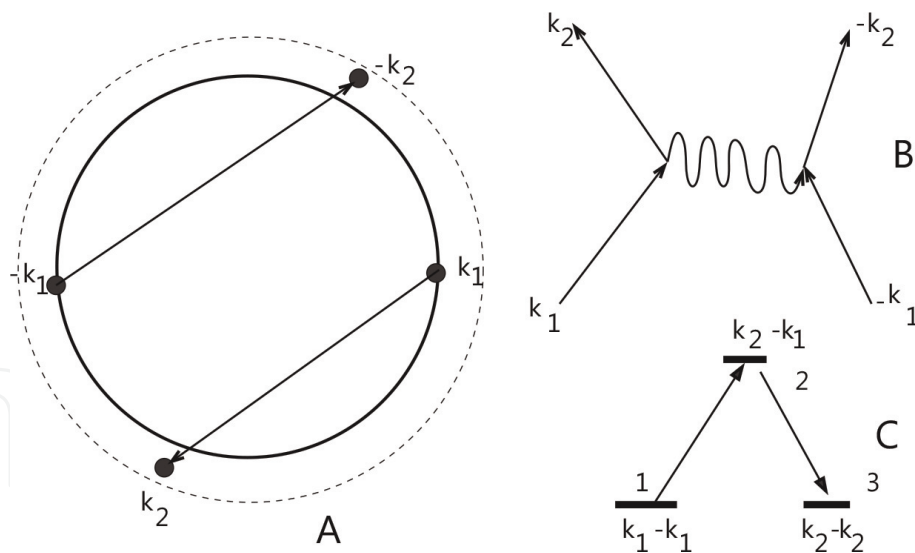
Figure 6.
(A) Depiction of the Fermi sphere and how electron pair $k_1, -k_1$ at Fermi sphere scatters to $k_2, -k_2$ at the Fermi sphere. (B) How this is mediated by exchange of a phonon in a Feynman diagram. (C) A three-level system that captures the various transitions involved in this process.

by electron $-k_1$ which absorbs this oscillation and is thrown back to momentum $-k_2$. The total momentum is conserved in the process. This is depicted in **Figure 6A**. The corresponding Feynman diagram for this process is shown in **Figure 6B**. The above process where two electrons interact with exchange of phonon can be represented as a three-level atomic system. Level 1 is the initial state of the electrons $k_1, -k_1$, level 3 is the final state of the electrons $k_2, -k_2$ and the level 2 is the intermediate state $k_2, -k_1$. There is a transition with strength $\Omega = \hbar d$ between levels 1 and 2 involving emission of a phonon and a transition with strength Ω between levels 2 and 3 involving absorption of a phonon. Let E_1, E_2, E_3 be the energy of the three levels. Since pairs are at Fermi surface, $E_1 = E_3$. The state of the three-level system evolves according to the Schrödinger equation:

$$\dot{\psi} = \frac{-i}{\hbar} \begin{bmatrix} E_1 & \Omega & 0 \\ \Omega^* & E_2 & \Omega^* \\ 0 & \Omega & E_1 \end{bmatrix} \psi. \tag{2}$$

We proceed into the interaction frame of the natural Hamiltonian (system energies) by transformation

$$\phi = \exp\left(\frac{it}{\hbar} \begin{bmatrix} E_1 & 0 & 0 \\ 0 & E_2 & 0 \\ 0 & 0 & E_1 \end{bmatrix}\right) \psi. \tag{3}$$

This gives for $\Delta E = E_2 - E_1$

$$\dot{\phi} = \frac{-i}{\hbar} \underbrace{\begin{bmatrix} 0 & \exp\left(-\frac{i}{\hbar}\Delta E\ t\right)\Omega & 0 \\ \exp\left(\frac{i}{\hbar}\Delta E\ t\right)\Omega^* & 0 & \exp\left(\frac{i}{\hbar}\Delta E\ t\right)\Omega^* \\ 0 & \exp\left(-\frac{i}{\hbar}\Delta E\ t\right)\Omega & 0 \end{bmatrix}}_{H(t)} \phi. \tag{4}$$

$H(t)$ is periodic with period $\Delta t = \frac{2\pi}{\Delta E}$. After Δt, the system evolution is

$$\phi(\Delta t) = \left(I + \int_0^{\Delta t} H(\sigma)d\sigma + \int_0^{\Delta t} \int_0^{\sigma_1} H(\sigma_1)H(\sigma_2)d\sigma_2 d\sigma_1 + ... \right)\phi(0). \qquad (5)$$

The first integral averages to zero, while the second integral

$$\int_0^{\Delta t} \int_0^{\sigma_1} H(\sigma_1)H(\sigma_2)d\sigma_2 d\sigma_1 = \frac{1}{2}\int_0^{\Delta t} \int_0^{\sigma_1} [H(\sigma_1), H(\sigma_2)]d\sigma_2 d\sigma_1. \qquad (6)$$

Evaluating it explicitly, we get for our system that second-order integral is

$$\frac{-i\Delta t}{\hbar} \begin{bmatrix} 0 & & \frac{|\Omega|^2}{E_1 - E_2} \\ 0 & 0 & 0 \\ \underset{\mathcal{M}}{\frac{|\Omega|^2}{E_1 - E_2}} & 0 & 0 \end{bmatrix}, \qquad (7)$$

which couples levels 1 and 3 and drives transition between them at rate $\mathcal{M} = \frac{\Omega^2}{E_1 - E_2}$.

Observe $E_1 = 2\epsilon_1$ and $E_3 = 2\epsilon_2$ and the electron energies $E_2 = \epsilon_1 + \epsilon_2 + \epsilon_d$, where $\epsilon_d = \hbar\omega_d$ is the energy of emitted phonon. We have $\epsilon_1 = \epsilon_2 = \epsilon$. Then, the transition rate between levels 1 and 3 is $\mathcal{M} = -\frac{\Omega^2}{\epsilon_d}$. Therefore, due to interaction mediated through lattice by exchange of phonons, the electron pair $k_1, -k_1$ scatters to $k_2, -k_2$ at rate $-\frac{\Omega^2}{\epsilon_d}$. The scattering rate is in fact $\Delta_b = -\frac{4\Omega^2}{\epsilon_d}$ as k_1 can emit to k_2 or $-k_2$. Similarly, $-k_1$ can emit to k_2 or $-k_2$, making it a total of four processes that can scatter $k_1, -k_1$ to $k_2, -k_2$.

How does all this help. Suppose $|k_1, -k_1\rangle$ and $|k_2, -k_2\rangle$ are only two states around. Then, a state like

$$\phi = \frac{|k_1, -k_1\rangle + |k_2, -k_2\rangle}{\sqrt{2}} \qquad (8)$$

has energy $2\epsilon + \Delta_b$. That has lower energy than the individual states in the superposition. Δ_b is the binding energy. Now, let us remember what is Ω. It comes from electron–phonon interaction. Let us pause, develop this a bit in the next section and come back to our discussion.

3. Electron-phonon collisions

Recall we are interested in studying how a BCS molecule scatters phonons. For this we first understand how a normal electron scatters of a thermal phonon. We also derive electron–phonon interaction (*Fröhlich*) Hamiltonian and show how to calculate Ω in the above. The following section is a bit lengthy as it develops ways to visualize how a thermal phonon scatters an electron.

Consider phonons in a crystalline solid. We first develop the concept of a phonon packet. To fix ideas, we start with the case of one-dimensional lattice potential. Consider a periodic potential with period a:

$$U(x) = \sum_{l=1}^{n} V(x - a_l) = \sum V(x - la),$$

where

$$V(x) = V_0 \cos^2\left(\frac{\pi x}{a}\right), \quad \frac{-a}{2} \leq x \leq \frac{a}{2} \tag{9}$$

$$= 0 \quad |x| \geq \frac{a}{2}. \tag{10}$$

The potential is shown in **Figure 7**.

Now, consider how potential changes when we perturb the lattice sites from their equilibrium position, due to lattice vibrations:

$$\Delta U(x) = \sum V'(x - a_l)\Delta a_l.$$

For a phonon mode with wavenumber k

$$\Delta a_l = A_k \frac{1}{\sqrt{n}} \exp(ika_l), \tag{11}$$

we have

$$\Delta U(x) = A_k \exp(ikx) \frac{1}{\sqrt{n}} \underbrace{\sum V'(x - a_l) \exp(-ik(x - a_l))}_{p(x)},$$

$$= A_k \exp(ikx) \frac{1}{\sqrt{n}} \underbrace{\sum V'(x - la) \exp(-ik(x - la))}_{p(x)},$$

where $p(x)$ is the periodic with period a. Note

$$V'(x) = -V_0 \frac{2\pi}{a} \sin\left(\frac{2\pi x}{a}\right), \quad \frac{-a}{2} \leq x \leq \frac{a}{2}$$

$$= 0 \, |x| \geq \frac{a}{2}.$$

Using Fourier series, we can write

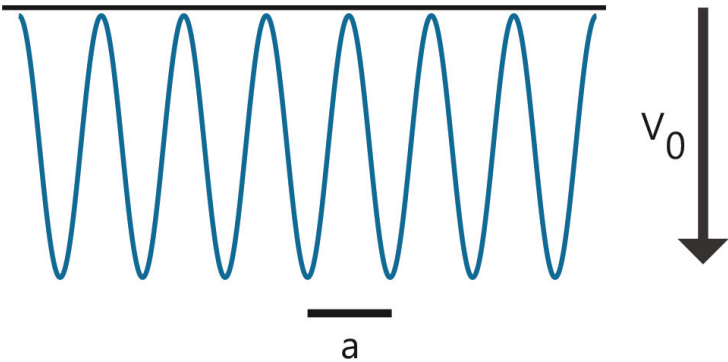$$p(x) = a_0 + \sum_r a_r \exp\left(i\frac{2\pi rx}{a}\right).$$

Figure 7.
Depiction of the periodic potential in Eq. (1).

We can determine a_0 by $a_0 = \frac{1}{a} \int_{-\frac{a}{2}}^{\frac{a}{2}} p(x) dx$, giving

$$a_0 = i \frac{V_0}{a} \int_{-\frac{a}{2}}^{\frac{a}{2}} \frac{2\pi}{a} \quad \sin\left(\frac{2\pi x}{a}\right) \sin(kx),$$

where $k = \frac{2\pi m}{na}$. This gives

$$a_0 = i \frac{2V_0}{a} \frac{1}{1 - \left(\frac{m}{n}\right)^2} \sin \frac{m\pi}{n}.$$

We do not worry much about a_r for $r \neq 0$ as these excite an electron to a different band and are truncated by the band-gap energy. Now, note that, using equipartition of energy, there is $k_B T$ energy per phonon mode, giving

$$A_k = \sqrt{\frac{k_B T}{m} \frac{1}{\omega_k}} = \sqrt{\frac{k_B T}{m} \frac{1}{\omega_d \sin\left(\frac{\pi m}{n}\right)}}, \tag{12}$$

where ω_d is the Debye frequency.

Then, we get

$$\Delta U(x) = \frac{i}{\sqrt{n}} \underbrace{\left(\frac{2V_0}{a} \sqrt{\frac{k_B T}{m} \frac{1}{\omega_d}}\right)}_{\overline{V}_0} \exp(ikx). \tag{13}$$

At temperature of T = 3 K and $\omega_d = 10^{13}$ rad/s, we have.
$\sqrt{\frac{k_B T}{m} \frac{1}{\omega_d}} \sim .03\,°\text{A}$; with a = 3 Å, we have

$$\Delta U \sim \frac{i}{\sqrt{n}} .01 V_0 \exp(ikx);$$

and with $V_0 = 10V$, we have

$$\Delta U \sim \frac{.1i}{\sqrt{n}} \exp(ikx) V.$$

We considered one phonon mode. Now, consider a phonon wave packet (which can also be thought of as a mode, localized in space) which takes the form

$$\Delta a_l = \frac{1}{n} \sum_k A_k \exp(ika_l),$$

where $k = m\Delta$ and $\Delta = \frac{2\pi}{na}$ and A_k as in Eq. (12). Then, the resulting deformation potential from Eq. (13) by summing over all phonon modes that build a packet becomes

$$\Delta U \sim \overline{V}_0 \frac{\sin^2\left(\frac{\pi x}{2a}\right)}{\left(\frac{\pi x}{2a}\right)}. \tag{14}$$

This deformation potential due to phonon wave packet is shown in **Figure 8**. The maximum value of the potential is around $\frac{\overline{V}_0}{\sqrt{2}}$.

3.1 Time dynamics and collisions

Of course phonons have a time dynamics given by their dispersion relation:

$$\Delta a_l(t) = \frac{1}{n} \sum_{k>0} (A_k \exp(ika_l) \exp(-i\omega_k t) + h.c). \tag{15}$$

With the phonon dispersion relation $\omega_k \sim vk$, where v is the velocity of sound, we get

$$\Delta U \sim \overline{V}_0 \frac{\sin^2\left(\frac{\pi(x-vt)}{2a}\right)}{\left(\frac{\pi(x-vt)}{2a}\right)}. \tag{16}$$

The deformation potential travels with velocity of sound and collides with an incoming electron. To understand this collision, consider a phonon packet as in Eq. (14) centred at the origin. The packet is like a potential hill. A electron comes along say at velocity v_g. If the velocity is high enough (kinetic energy $\frac{1}{2}mv_g^2 > \frac{e\overline{V}_0}{\sqrt{2}}$) to climb the hill, it will go past the phonon as in (b) in **Figure 9**, or else it will slide back, rebound of the hill and go back at the same velocity v_g as in (a) in **Figure 9**.
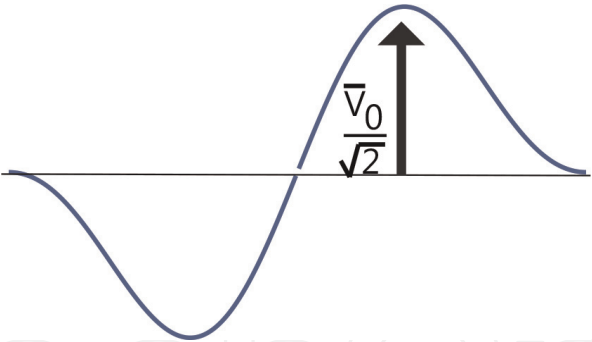

Figure 8.
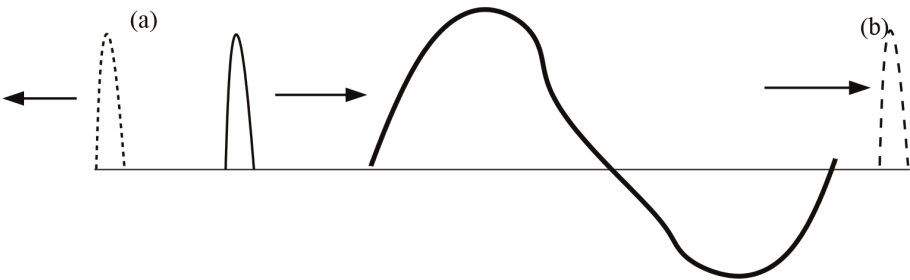*Depiction of the deformation potential in Eq. (14).*

Figure 9.
Depiction on how an incoming electron goes past the deformation potential (b); if its velocity is sufficient, else it slides back and rebounds as in (a).

In the above, we assumed phonon packet is stationary; however, it moves with velocity v. Now, consider two scenarios. In the first one, the electron and phonon are moving in opposite direction and collide. This is shown in **Figure 10**.

In the phonon frame the electron travels towards it with velocity $v_g + v$. If the velocity is high enough (kinetic energy $\frac{1}{2}m(v_g + v)^2 > \frac{e\overline{V}_0}{\sqrt{2}}$) to climb the hill, it will go past the phonon with velocity $v_g + v$ (the resulting electron velocity in lab frame is just v_g). Otherwise, it slides back, rebounds and goes back with velocity $v_g + v$ (the velocity in lab frame is $v_g + 2v$). Therefore, electron has gained energy:

$$\Delta E = mv_g v \qquad (17)$$

and by conservation of energy, the phonon has lost energy, lowering its temperature.

In the second case, electron and phonon are traveling in the same direction. This is shown in **Figure 11**. In the frame of phonon, electron travels towards the phonon with velocity $v_g - v$. If the velocity is high enough (kinetic energy $\frac{1}{2}m(v_g - v)^2 > \frac{e\overline{V}_0}{\sqrt{2}}$) to climb the hill, it will go past the phonon with velocity $v_g - v$. The velocity in lab frame is v_g. Otherwise, it slides back, rebounds and goes back with velocity $v_g - v$. Then, the velocity in lab frame is $v_g - 2v$. Therefore, electron has lost energy, and by conservation of energy, the phonon has gained energy, raising its temperature.

Thus, we have shown that electron and phonon can exchange energy due to collisions. Now, everything is true as in statistical mechanics, and we can go on to derive *Fermi-Dirac* distribution for the electrons [4–7].

All our analysis has been in one dimension. In two or three dimensions, the phonon packets are phonon tides (as in ocean tides). Let us fix ideas with two dimensions, and three dimensions follow directly. Consider a two-dimensional periodic potential with period a:

$$U(x,y) = \sum_{lm} V(x - a_l, y - a_m) = \sum_{lm} V(x - la, y - ma). \qquad (18)$$

$$
\begin{aligned}
V(x,y) &= V_0 \cos^2\left(\frac{\pi x}{a}\right)\cos^2\left(\frac{\pi y}{a}\right), \quad \frac{-a}{2} \leq x, y \leq \frac{a}{2} \\
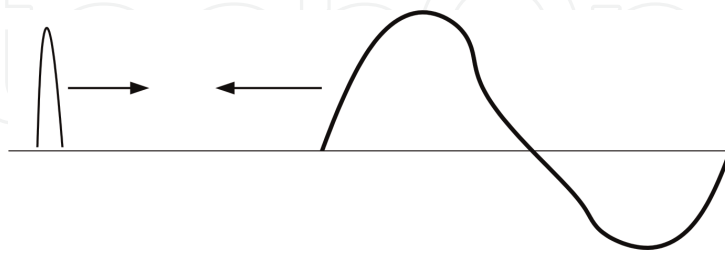&= 0 \quad |x|, |y| \geq \frac{a}{2}.
\end{aligned}
\qquad (19)
$$

Figure 10.
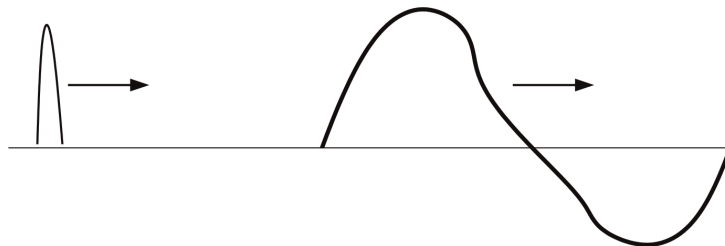*Depiction on how an electron and phonon traveling towards each other collide.*

Figure 11.
Depiction on how an electron and phonon traveling in same direction collide.

Now, consider how potential changes when we perturb the lattice sites from their equilibrium position, due to lattice vibrations:

$$\Delta U(x,y) = \sum_{lm} V_x(x - a_l, y - a_m)\Delta a_l + V_y(x - a_l, y - a_m)\Delta a_m.$$

Let us consider phonons propagating along x direction. Then, Δa_l constitutes longitudinal phonons, while Δa_m constitutes transverse phonons. Transverse phonons do not contribute to deformation potential as can be seen in the following. Let us focus on the transverse phonons. Then,

$$\Delta a_m = A_k \frac{1}{\sqrt{n}} \exp(ik_x a_l). \tag{20}$$

We have due to Δa_m

$$\Delta U(x,y) = A_k \exp(ik_x x)\frac{1}{\sqrt{n}}\underbrace{\sum V_y(x - a_l, y - a_m)\exp(-ik(x - a_l))}_{p(x,y)},$$

where $p(x,y)$ is the periodic with period a.
Note

$$V_y(x,y) = -V_0\frac{2\pi}{a}\ \sin\left(\frac{2\pi y}{a}\right)\cos\left(\frac{\pi x}{a}\right)^2, \quad \frac{-a}{2} \leq x, y \leq \frac{a}{2}$$

$$= 0 \quad |x|, |y| \geq \frac{a}{2}.$$

Using Fourier series, we can write

$$p(x,y) = a_0 + \sum_{r,s} a_{rs} \exp\left(i\left(\frac{2\pi r x}{a} + \frac{2\pi s y}{a}\right)\right).$$

We can determine a_0 by $a_0 = \frac{1}{a^2}\int_{-\frac{a}{2}}^{\frac{a}{2}}\int_{-\frac{a}{2}}^{\frac{a}{2}} p(x,y)dxdy$, giving $a_0 = 0$. Hence, transverse phonons do not contribute. The contribution of longitudinal phonons is same as in 1D case. As before consider a wave packet of longitudinal phonons propagating along x direction:

$$\Delta a_l = \frac{1}{n}\sum_k A_k \exp(ika_l),$$

which gives us a deformation potential as before:

$$\Delta U(x,y) \sim \overline{V}_0 \frac{\sin^2\left(\frac{\pi(x-vt)}{2a}\right)}{\left(\frac{\pi(x-vt)}{2a}\right)}, \tag{21}$$

which is same along y direction and travels with velocity v along the x direction except now the potential is like a tide in an ocean, as shown in **Figure 12**.

Since deformation potential is a tide, electron–phonon collisions do not have to be head on; they can happen at oblique angles, as shown in **Figure 13** in a top view (looking down). The velocity of electron parallel to tide remains unchanged, while velocity perpendicular to tide gets reflected. If the perpendicular velocity is large enough, the electron can jump over the tide and continue as shown by a dotted line in **Figure 13**. Imagining the tide in three dimensions is straightforward. In three
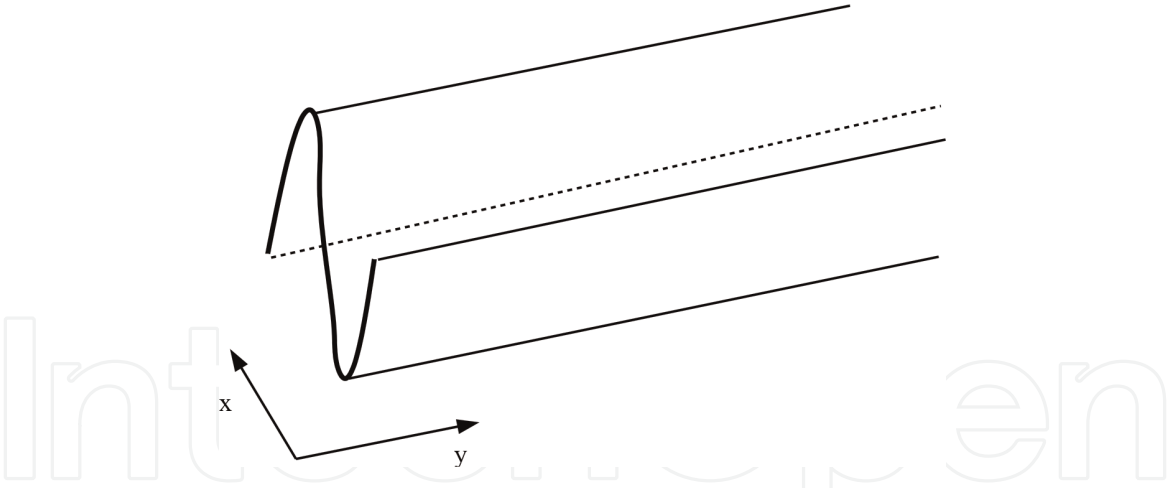
Figure 12.
Depiction of the deformation potential tide as shown in Eq. (21).
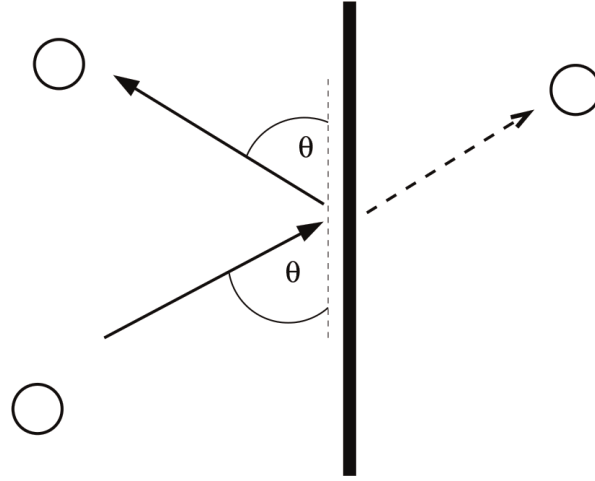

Figure 13.
The top view collision of an electron with a deformation potential tide at an angle θ.

dimensions, the deformation potential takes the form a wind gust moving in say x direction.

We described how a normal electron scatters phonons. Now, let us go back to our discussion on electron-phonon interaction and recall a phonon $\exp(ikx)$ which produces a deformation potential $\Delta U(x)$ as in Eq. 13. Now in three dimensions, it is

$$\Delta U(x) = \frac{i}{\sqrt{n^3}} \frac{V_0}{a} A_k (\exp(ikx) \exp(-i\omega_k t) - h.c), \tag{22}$$

where n^3 is the number of lattice points.

Using $\frac{1}{2} M \omega_k^2 A_k^2 = n_k \hbar \omega_k$ (there are n_k quanta in the phonon), where M is the mass of ion, ω_k phonon frequency and replacing A_k, we get

$$\Delta U(x) = \frac{i}{\sqrt{n^3}} \underbrace{\frac{V_0}{a} \sqrt{\frac{2\hbar}{M\omega_k}}}_{c} (\sqrt{n_k} \exp(ikx) \exp(-i\omega_k t) - h.c). \tag{23}$$

Thus, electron-phonon coupling Hamiltonian is of form

$$\underbrace{\frac{c}{\sqrt{n^3}}}_{\Omega} \, i\big(b \exp(ikx) - b^\dagger \exp(-ikx)\big), \tag{24}$$

where b, $b^\dagger$ are the annihilation and creation operators for phonon.

Using a cosine potential with $V_0 \sim 10$ V, we can approximate Coulomb potential. Then, with $a \sim 3A°$ and $M \sim 20$ proton masses, we have $c \sim 1$ V.

We just derived an expression for the electron-phonon interaction (*Fröhlich*) Hamiltonian in Eq. (24) and showed how to calculate the constant c.

We said there are only two states, $|k_1, -k_1\rangle$ and $|k_2, -k_2\rangle$. In general we have for $i = 1, ..., \mathcal{N}$, $|k_i, -k_i\rangle$ states on the Fermi sphere as shown in **Figure 14A**, and if we form the state

$$\phi = \frac{1}{\sqrt{N}} \sum_i |k_i, -k_i\rangle, \tag{25}$$

it has energy $2\epsilon + (\mathcal{N} - 1)\Delta_b$.

The states do not have to be exactly on a Fermi surface as shown in **Figure 14A**; rather, they can be in an annulus around the Fermi sphere as shown in **Figure 14B**. When $|k_1, -k_1\rangle$ and $|k_2, -k_2\rangle$ are not both on the Fermi surface (rather in an annulus) such that the energy of $|k_1, -k_1\rangle$ is $E_1 = 2\epsilon_1$ and the energy of $E_3 = |k_2, -k_2\rangle$ is $2\epsilon_2$, with $\varepsilon_1 \neq \varepsilon_2$, then the formula of scattering amplitude (as shown in detail below) is modified to $\Delta_b = \frac{4\epsilon_d \Omega^2}{\Delta\epsilon^2 - \epsilon_d^2}$, where $\epsilon_1 - \epsilon_2 = \Delta\epsilon = \hbar\Delta\omega$. As long as $\Delta\omega < \omega_d$, in BCS theory, we approximate $\Delta_b \sim -\frac{4\Omega^2}{\epsilon_d}$. Therefore, if we take an annulus in **Figure 14B** to be of width ω_d, we get a total number of states in the annulus $\mathcal{N}$ to be $\frac{\mathcal{N}}{n^3} \sim \frac{\omega_d}{\omega_F}$, where n^3 is the total number of k points in the Fermi sphere and $\epsilon_F = \hbar\omega_F$ is the Fermi energy. This gives a binding energy $\Delta_b = \sim \frac{c^2}{\epsilon_F}$. With the Fermi energy $\epsilon_F \sim 10$ eV, the binding energy is $\sim$meV. Thus, we have shown how phonon-mediated interaction helps us bind an electron pair with energy $\sim$meV.
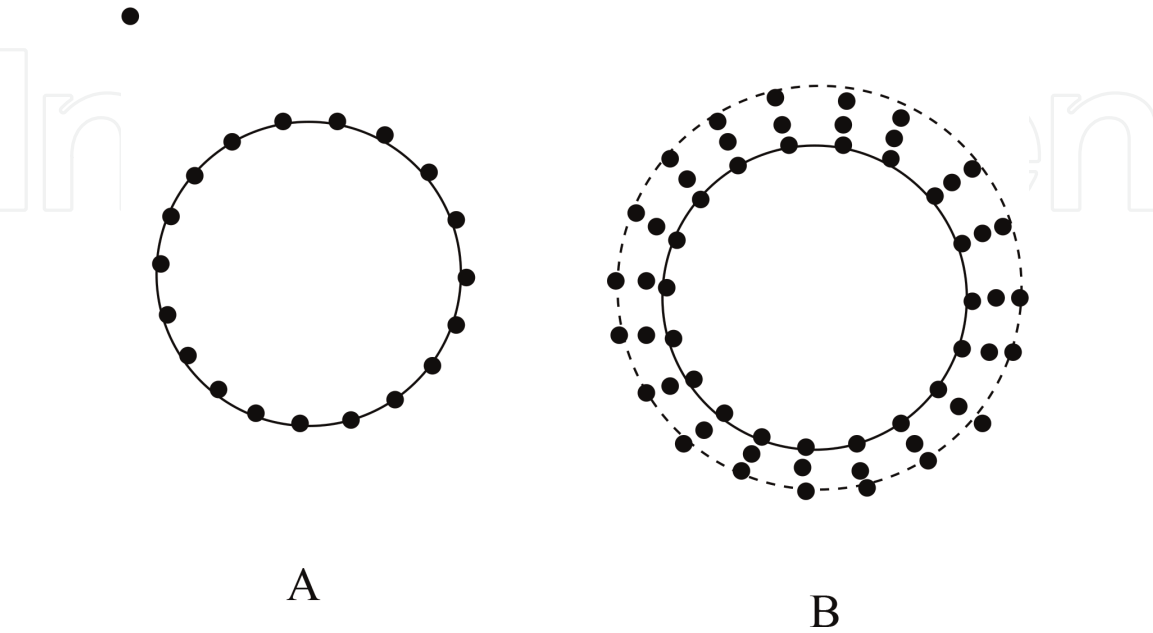

Figure 14.
(A) Electron pairs on the fermi surface and (B) electron pairs in an annulus around the fermi surface.

This paired electron state is called Cooper pair. Now, the plan is we bind many electrons and make a big molecule called BCS ground state.

But before we proceed, a note of caution is in order when we use the formula $\Delta_b = \frac{4\epsilon_d \Omega^2}{\Delta\epsilon^2 - \epsilon_d^2}$. For this we return to phonon scattering of $|k_1, -k_1\rangle$ and $|k_2, -k_2\rangle$. Consider when $E_1 \neq E_3$. Observe $E_1 = 2\epsilon_1 = 2\hbar\omega_1$, $E_3 = 2\epsilon_2 = 2\hbar\omega_2$, $E_2 = \epsilon_1 + \epsilon_2$ and $\hbar\omega_d$ is the energy of the emitted phonon. All energies are with respect to Fermi surface energy ϵ_F. The state of the three-level system evolves according to the Schrödinger equation:

$$\dot{\psi} = -i \begin{bmatrix} 2\omega_1 & d\exp(-i\omega_d t) & 0 \\ d\exp(i\omega_d t) & \omega_1 + \omega_2 & d\exp(i\omega_d t) \\ 0 & d\exp(-i\omega_d) & 2\omega_2 \end{bmatrix} \psi. \tag{26}$$

We proceed into the interaction frame of the natural Hamiltonian (system energies) by transformation:

$$\phi = \exp\left(it \begin{bmatrix} 2\omega_1 & 0 & 0 \\ 0 & \omega_1 + \omega_2 & 0 \\ 0 & 0 & 2\omega_2 \end{bmatrix} \right) \psi. \tag{27}$$

This gives for $\Delta E_1 = \omega_d - (\omega_1 - \omega_2)_{\Delta\omega}$ and $\Delta E_2 = \omega_d + \Delta\omega$

$$\dot{\phi} = -i \begin{bmatrix} 0 & \exp(-i\Delta E_1\ t)d & 0 \\ \exp(i\Delta E_1\ t)d & 0 & \exp(i\Delta E_2\ t)d \\ 0 & \exp(-i\Delta E_2\ t)d & 0 \end{bmatrix} \phi. \tag{28}$$

$$\underbrace{}_{H(t)}$$

We evaluate the effective evolution of $H(t)$ in period $\Delta t = \frac{2\pi}{\omega_d}$. After Δt, the system evolution is

$$\phi(\Delta t) = \exp\left(\underbrace{\int_0^{\Delta t} H(\sigma)d\sigma + \frac{1}{2}\int_0^{\Delta t}\left[H(\sigma_1), \int_0^{\sigma_1} H(\sigma_2)d\sigma_2 \right]d\sigma_1}_{\overline{H}\ \Delta t} \right) \phi(0). \tag{29}$$

Let us calculate $\overline{H}_{12}$. Assuming $|\Delta\omega| \ll \omega_d$, then

$$\overline{H}_{12} = \frac{-i}{\Delta t}\int_0^{\Delta t} \exp(-i\Delta E_1\ t)d = i\frac{\Delta\omega}{\omega_d}d. \tag{30}$$

Similarly

$$\overline{H}_{23} = \frac{-i}{\Delta t}\int_0^{\Delta t} \exp(-i\Delta E_2\ t)d = -i\frac{\Delta\omega}{\omega_d}d, \tag{31}$$

and finally

$$\overline{H}_{13} = \frac{-d^2}{2\Delta t}\left\{\int_0^{\Delta t}\exp\left(-i\Delta E_1\ t\right)\int_0^{\tau}\exp\left(i\Delta E_2\ t\right) - \int_0^{\Delta t}\exp\left(i\Delta E_2\ t\right)\int_0^{\tau}\exp\left(-i\Delta E_1\ t\right)\right\}$$

$$= \frac{id^2}{2\Delta t}\left(\frac{1}{\omega_d + \Delta\omega} + \frac{1}{\omega_d - \Delta\omega}\right)\int_0^{\Delta t}\exp\left(i2\Delta\omega\ t\right) = -i\frac{-d^2\omega_d\ \exp\left(i\Delta\omega\Delta t\right)}{\omega_d^2 - \Delta\omega^2}$$

$$\sim -i\frac{-d^2\exp\left(i\Delta\omega\Delta t\right)}{\omega_d}.$$

Then, from Eq. (27), we get

$$\psi(\Delta T) = \exp\left(-i\Delta\begin{bmatrix}2\omega_1 & 0 & 0\\ 0 & \omega_1 + \omega_2 & 0\\ 0 & 0 & 2\omega_2\end{bmatrix}\right)\exp\left(\overline{H}\Delta t\right)\ \psi(0) = \exp\left(H^{eff}\Delta t\right)\psi(0),$$

(32)

where

$$H^{eff} = -i\begin{bmatrix}2\omega_1 & -\frac{\Delta\omega}{\omega_d}d\exp\left(\frac{i}{2}\Delta\omega\Delta t\right) & \frac{-d^2}{\omega_d}\\ -\frac{\Delta\omega}{\omega_d}d\exp\left(-\frac{i}{2}\Delta\omega\Delta t\right) & \omega_1 + \omega_2 & \frac{\Delta\omega}{\omega_d}d\exp\left(-\frac{i}{2}\Delta\omega\Delta t\right)\\ \frac{-d^2}{\omega_d} & \frac{\Delta\omega}{\omega_d}d\exp\left(\frac{i}{2}\Delta\omega\Delta t\right) & 2\omega_2\end{bmatrix}.$$

(33)

Observe in the above the term H_{13}^{eff} gives us the attractive potential responsible for superconductivity [3]. We say the electron pair $k_1,\ -k_1$ scatters to $k_2,\ -k_2$ at rate $-\frac{d^2}{\omega_d}$. But observe $d \ll \Delta\omega$, that is, term H_{13}^{eff} is much smaller than terms H_{12}^{eff} and H_{23}^{eff}: then, how are we justified in neglecting these terms. This suggests our calculation of scattering into an annulus around the Fermi surface requires caution and our expression for the binding energy may be high as binding deteriorates in the presence of offset. However, we show everything works as expected if we move to a wave-packet picture. The key idea is what we call *offset averaging*, which we develop now.

We have been talking about electron waves in this section. Earlier, we spent considerable time showing how electrons are wave packets confined to local potentials. We now look for phonon-mediated interaction between wave packets. A wave packet is built from many k-states (k-points). These states have slightly different energies (frequencies) which make the packet moves. We call these different frequencies *offsets* from the centre frequency. Denote $\exp\left(ik_0x\right)p(x)$ as a wave packet centred at momentum k_0. The key idea is that due to local potential, the wave packet shuttles back and forth and comes back to its original state. This means on average that the energy difference between its k-points averages and the whole packet just evolved with frequency $\omega(k_0)$. We may say the packet is *stationary* in the well, evolving as $\exp\left(ik_0x\right)p(x) \rightarrow \exp\left(-i\omega(k_0)t\right)\exp\left(ik_0x\right)p(x)$. **Figure 15** picturizes the offsets getting averaged by showing wave packets standing in the local potential. All we are saying is that now the whole packet has energy ϵ_0. So now, we can study how packet pair (at fermi surface) centred at $k_1,\ -k_1$ scatters to $k_2,\ -k_2$. This is shown in **Figure 16A**. The scattering is through a phonon packet with width localized to the local well. Let us say our electron packet width is Debye frequency ω_d. If there are N k-points in a packet, the original scattering rate Δ_b gets modified
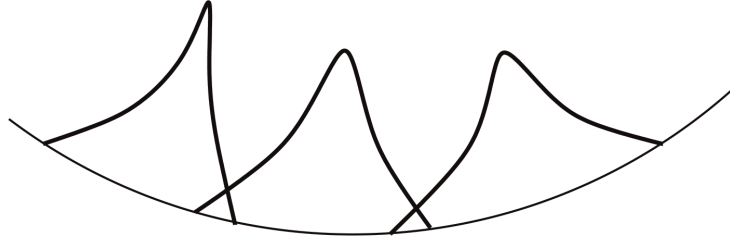
Figure 15.
The offsets getting averaged by showing wave packets standing in the local potential, bound by phonon-mediated interaction. Offset average so effectively packets are standstill; they do not move.

to $N\Delta_b$. If there are p packet pairs at the Fermi surface as shown in **Figure 16A**, then the state formed from superposition of packet pairs

$$\phi = \frac{1}{\sqrt{p}} \sum_i |k_i, -k_i\rangle \tag{34}$$

has binding energy $pN\Delta_b$. What is Np though is really just a $\mathcal{N}$ number of points in the annulus around the Fermi surface which we counted earlier. Hence, we recover the binding energy we derived between electrons earlier, but now it is binding of packets. Really, this way we do not have to worry about offsets when we bind; in packet land they average in local potential.

The wave packet in a potential well shuttles back and forth, which averages the offsets $\omega_i - \omega_j$ to zero. Then, the question of interest is how fast do we average these offsets compared to packet width which we take as Debye frequency ω_d. For s orbitals or waves, the bandwidth is $\sim$10 eV giving Fermi velocity of 10^5 m/s, which for a characteristic length of the potential well as $\sim$300 Å, corresponds to a packet shuttling time of around $\sim 10^{-13}$s, which is same as the Debye frequency ω_d, so we may say we average the offsets in a packet. By the time offsets have evolved significantly, the packet already returns to its original position, and we may say there are no offsets.

We saw how two electrons bind to form a Cooper pair. However, for a big molecule, we need to bind many electrons. How this works will be discussed now. The basic idea is with many electrons; we need space for electron wave packets to scatter to. For example, when there was only one packet pair at the Fermi surface, it could scatter into all possible other packet pairs, and we saw how we could then form a superposition of these states. Now, suppose we have $2p$ packet pairs possible on the Fermi surface. We begin with assuming p of these are occupied with
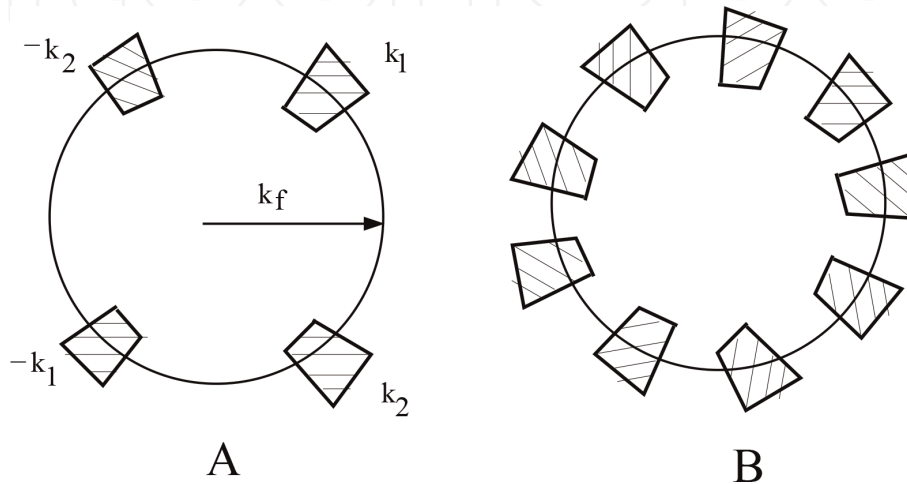

Figure 16.
(A) Packet pairs k_1, $-k_1$ and k_2, $-k_2$ on the Fermi surface and (B) many such pairs.
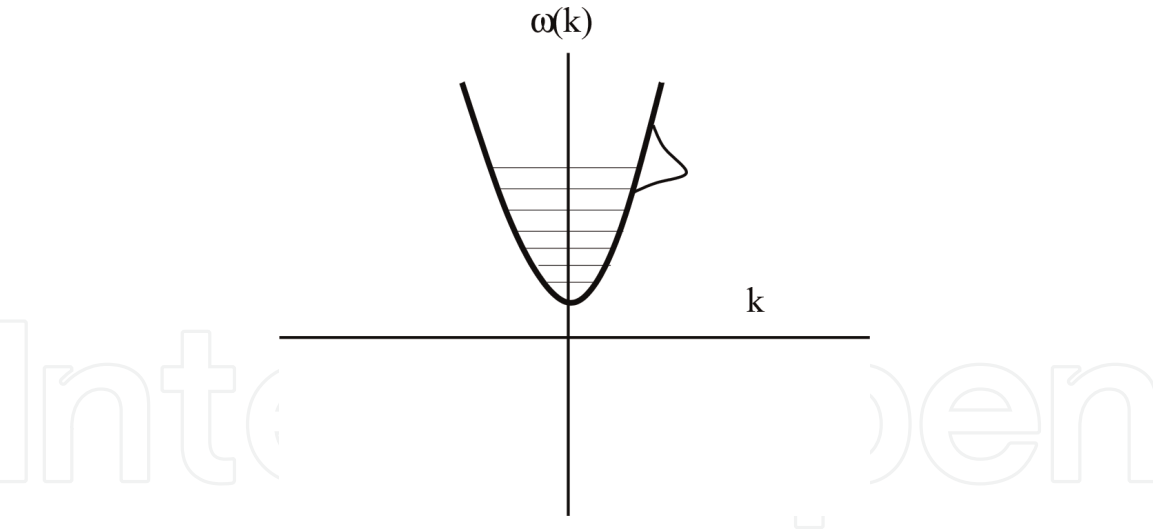
$$\omega(k)$$

$$k$$

Figure 17.
Packets at the Fermi surface that has twice the number of k-states as electrons. This means half the packet sites will be empty.

electrons and remaining p empty. This way we create space for the p pairs to scatter into; otherwise, if all are full, how will we scatter? How do these empty spaces come about? We just form packets with twice the bandwidth as there are electrons. Then, half of these packets are empty as shown in **Figure 17**.

4. BCS ground state

Let k_F denote wavevector radius of the Fermi sphere. We describe electron wave packets formed from k-points (wavevectors) near the Fermi sphere surface. **Figure 18** shows the Fermi sphere with surface as thick circle and an annulus of thickness ω_d (energy units) shown in dotted lines. Pockets have **n**, k-points in radial direction ($\frac{n}{2}$ inside and same outside the Fermi sphere) and **m²** points in the tangential direction. **Figure 18** shows such a pocket enlarged with k-points shown in

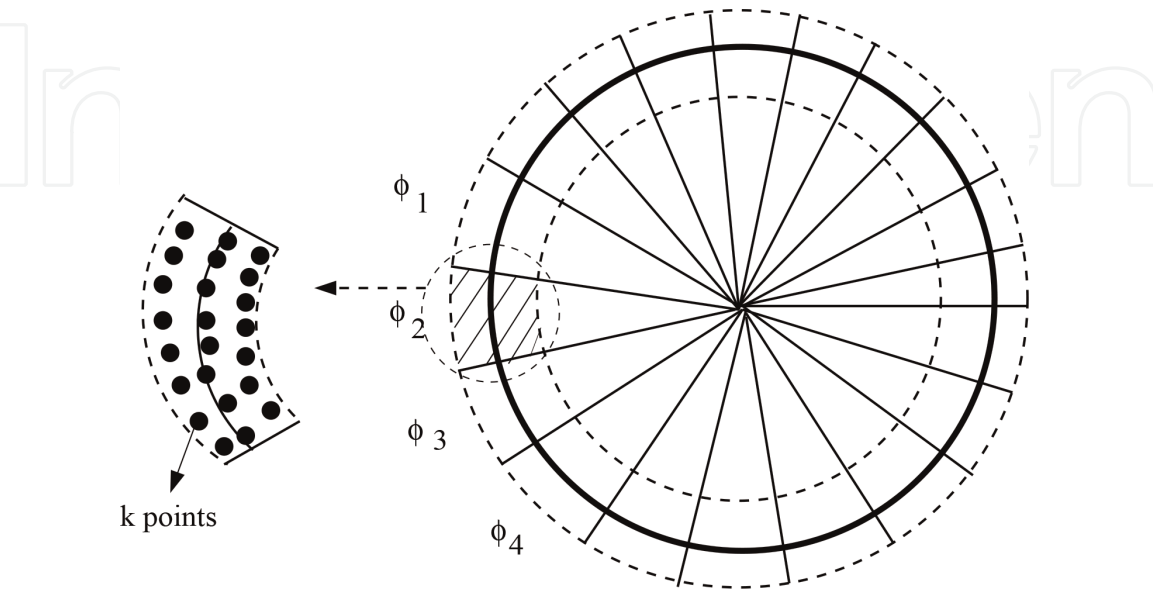$$\phi_1$$
$$\phi_2$$
$$\phi_3$$
$$\phi_4$$

k points

Figure 18.
Depiction of the Fermi sphere with surface as a thick circle and an annulus of thickness ω_d (energy units) shown in dotted lines. Pockets with k-points are shown in black dots. Superposition of these k-points in a pocket forms a wave packet.

black dots. We assume there are $4p$ such pockets with $N = \mathbf{nm}^2$ points in each pocket. In pocket s, we form the function

$$\phi_s(r) = \frac{1}{\sqrt{N}} \sum_j \exp(ik_j \cdot r) \tag{35}$$

ϕ_s has characteristic width a. From N points in a pocket, we can form N such functions by displacing ϕ_s to $\phi_s(r - ma)$, and putting these functions uniformly spaced over the whole lattice in their local potential wells. Thus, each pocket gives N wave packets orthogonal as they are nonoverlapping and placed uniformly over the lattice in their local potential wells. Furthermore, ϕ_s and $\phi_{s'}$ are orthogonal as they are formed from mutually exclusive k-points. The wave packet ϕ_s moves with a group velocity v, which is the Fermi velocity in a radial direction to the pocket from which it is formed. From wave packet ϕ_s and its antipodal packet ϕ_{-s}, we form the joint wave packet:

$$\Phi_s(r_1, r_2) = \phi_s(r_1)\phi_{-s}(r_2). \tag{36}$$

As we will see soon, Φ_s will be our Cooper pair.

As shown in last section, the Cooper pair Φ_s scatters to $\Phi_{s'}$ with rate $\mathcal{M} = -\frac{4d^2N}{\omega_d}$. Now, we study how to form BCS state with many wave packets. We present a counting argument. Observe ϕ_s is made of N k-points, and hence by displacement of ϕ_s, we have N nonoverlapping lattice sites (potential wells) where we can put copies of ϕ_s as described in Section 4. However of the N k-points, only $\frac{N}{2}$ are inside the Fermi sphere so we only have only $\frac{N}{2}$ wave packets. Therefore, $\frac{1}{2}$ of the wave-packet sites are empty. Hence, of the $2p$ possible Cooper pairs, only p are filled and p are not present. Hence, when Φ_s scatters to $\Phi_{s'}$, we have p choices for s'. Then, we can form a joint state of Cooper pairs present and write it as $\Phi_{i_1}\Phi_{i_2}...\Phi_{i_p}$. Doing a superposition of such states, we get the superconducting state:

$$\Psi = \sum \Phi_{i_1}\Phi_{i_2}...\Phi_{i_p}. \tag{37}$$

The binding energy of this state is $-\frac{4\hbar d^2Np^2}{\omega_d}$ as each index in Ψ scatters to p states. Since $4pN$ are the total k-points in the annulus surrounding the Fermi surface. We have $\Omega = \frac{c}{\sqrt{n^3}}$ where c is of order 1 eV and n^3 is the total number of lattice sites in the solid. Then, $\frac{4Np}{n^3} \sim \frac{\omega_d}{\omega_F}$. Thus, the binding energy is $-pc\frac{c}{\hbar\omega_F}$ ($c\frac{c}{2\hbar\omega_F}$ per wave packet/ electron). The Fermi energy $\hbar\omega_F$ is of order 10 eV, while $\hbar\omega_d \sim .1$ eV. Thus, binding energy per wave packet is of order .05 eV. The average kinetic energy of the wave packet is just the Fermi energy ϵ_F as it is made of superposition of $\frac{N}{2}$ points inside and $\frac{N}{2}$ points outside the Fermi sphere. If the wave packet was just formed from k-point inside the Fermi surface, its average energy would be $\epsilon_F - \frac{\hbar\omega_d}{4}$. Thus, we pay a price of $\frac{\hbar\omega_d}{4} \sim .025$ eV per wave packet; when we form our wave packet out of N k-points, half of which are outside the Fermi sphere. Thus, per electron wave packet, we have a binding energy of $\sim.025$ eV around 20 meV. Therefore, forming a superconducting state is only favorable if $c\frac{c}{\hbar\omega_F} > \frac{\hbar\omega_d}{4}$. Observe if c is too small, then forming the superconducting state is not useful, as the gain of binding energy is offsetted by the price we pay in having wave packets that have excursion outside the Fermi surface.

Next, we study how low-frequency thermal phonons try to break the BCS molecule. The electron wave packet collides with the phonon and gets deflected,

which means the Cooper pair gets broken. Then, the superconducting state constitutes $p - 1$ pairs and damaged pair. Each term in the state in Eq. (37) will scatter to $p(p-1)$ states, and the binding energy is $-\frac{4\hbar d^2 N p(p-1)}{\omega_d}$. The total binding energy has reduced by $\Delta = \frac{4\hbar d^2 N p}{\omega_d}$, the superconducting gap. The phonon with which the superconducting electron collides carries an energy $k_B T$. When this energy is less than Δ, the electron cannot be deflected and will not scatter as we cannot pay for the increase of energy. Therefore, superconducting electrons do not scatter phonons. However, this is not the whole story as the phonon can deflect the electron slightly from its course and over many such collisions break the Cooper pair; then, the energy budget Δ is paid in many increments of $k_B T$. These are small angle scattering events. Thus, there will be a finite probability q that a Cooper pair is broken, and we say we have excited a **Bogoliubov** [8]. This probability can be calculated using Boltzmann distribution. In a superconducting state with $2p$, wave packets on average $2pq$ will be damaged/deflected. This leaves only $p' = p(1 - 2q)$ good pairs which give an average energy per pair to be $(1 - 2q)\Delta$. The probability that the superconducting electron will be deflected of phonon is

$$q = \frac{\exp\left(-(1-2q)\Delta/k_B T\right)}{1 + \exp\left(-(1-2q)\Delta/k_B T\right)},$$

which gives

$$\ln\left(\frac{1}{q} - 1\right) = \frac{(1-2q)\Delta}{k_B T}. \tag{38}$$

When $k_B T_c = \Delta$, the above equation gives $q = \frac{1}{2}$ and gap $(1 - 2q)\Delta$ goes to zero. T_c is the critical temperature where superconducting transition sets in.

5. Molecular orbitals of BCS states

We now come to interaction of neighboring BCS molecules. In our picture of *local potentials*, we have electron wave packets in each potential well that are coupled as pairs by phonon to form the BCS ground state. What is important is that there is a BCS ground state in each potential well. When we bring two such wells in proximity, the ground state wave functions overlap, and we form a molecular orbital between these BCS orbitals. This is shown in **Figure 19**.

If Φ_1 and Φ_2 are the orbitals of Cooper pair in individual potential wells, then the overlap creates a transition $d = \langle \Phi_1 | 2eU | \Phi_2 \rangle$, where U is the potential well, with $2e$ coming from the electron pair charge. Then, the linear combination of atomic orbital (LCAO) $a\Phi_1 + b\Phi_2$ evolves as
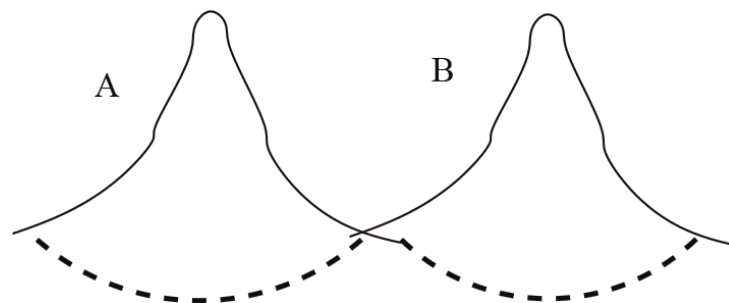

Figure 19.
Depiction of two BCS ground states in local potential wells separated in a weak link.

$$\hbar \frac{d}{dt} \begin{bmatrix} a \\ b \end{bmatrix} = -i \begin{bmatrix} \epsilon_1 - 2\Delta & d \\ d & \epsilon_2 - 2\Delta \end{bmatrix} \begin{bmatrix} a \\ b \end{bmatrix} \tag{39}$$

where ϵ_1, ϵ_2 is the Fermi energy of the electron pair in two orbitals. $\epsilon_1 = \epsilon_2$ unless we apply a voltage difference v between them; then, $\epsilon_1 - \epsilon_2 = v$. Let us start with $v = 0$ and $\begin{bmatrix} a \\ b \end{bmatrix} = \begin{bmatrix} 1 \\ 1 \end{bmatrix}$, and then nothing happens, but when there is phase difference $\begin{bmatrix} a \\ b \end{bmatrix} = \begin{bmatrix} 1 \\ \exp(i\phi) \end{bmatrix}$, then $\begin{bmatrix} a \\ b \end{bmatrix}$ evolves and we say we have supercurrent $I \propto \sin \phi$ between two superconductors. This constitutes the Josephson junction (in a Josephson junction, there is a thin insulator separating two BCS states or superconductors). Applying v generates a phase difference $\frac{d\phi}{dt} \propto v$ between the two orbitals which then evolves under d.

We talked about two BCS states separated by a thin insulator in a Josephson junction. In an actual superconductor, we have an array (lattice) of such localized BCS states as shown in **Figure 20**. Different phases ϕ_i induce a supercurrent as in Josephson junction.

If Φ_i denotes the local Cooper pairs, then their overlap creates a transition $d = \langle \Phi_i | 2eU | \Phi_{i+1} \rangle$, where U is the potential well, with $2e$ coming from the electron pair charge. Then, the LCAO $\sum a_i \Phi_i$ evolves as

$$\hbar \frac{d}{dt} \begin{bmatrix} a_1 \\ \vdots \\ a_n \end{bmatrix} = -i \begin{bmatrix} \epsilon_1 - 2\Delta & d & 0 \\ d & \ddots & \vdots \\ & d & \epsilon_n - 2\Delta \end{bmatrix} \begin{bmatrix} a_1 \\ \vdots \\ a_n \end{bmatrix} \tag{40}$$

where $\epsilon_i = \epsilon_0$ is the Fermi energy of the electron pair in BCS state Φ_i. ϵ_i is same unless we apply a voltage difference v to the superconductor. Eq. 40 is the tight-binding approximation model for superconductor.

What we have now is a new lattice of potential wells as shown in **Figure 20** with spacing of $b \sim 300$ Å as compared to the original lattice of $a \sim 3$ Å, which means 100 times larger. We have an electron pair at each lattice site. The state

$$\begin{bmatrix} a_1 \\ \vdots \\ a_n \end{bmatrix} = \frac{1}{\sqrt{n}} \begin{bmatrix} 1 \\ \vdots \\ 1 \end{bmatrix} \tag{41}$$

is the ground state of new lattice (Eq. 40). A state like

$$\begin{bmatrix} a_1 \\ \vdots \\ a_n \end{bmatrix} = \frac{1}{\sqrt{n}} \begin{bmatrix} \exp(ikx_1) \\ \vdots \\ \exp(ikx_n) \end{bmatrix}$$
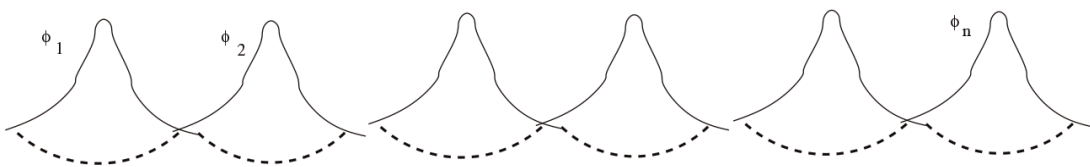

Figure 20.
Depiction of array of local BCS states in local potential wells with different phases.

has a momentum and constitutes the supercurrent. It has energy
$\epsilon_k = \epsilon_0 - 2\Delta + 2d \cos kb$.

In the presence of electric field E, we get on the diagonal of RHS of Eq. 40, additional potential eEx_i. How does ϕ_k evolve under this field? Verify with $k(t) = k - \frac{eEt}{\hbar}$; $\phi_{k(t)}$ is a solution with eigenvalue $\epsilon_{k(t)}$. In general, in the presence of time varying $E(t)$, we have $k(t) = k - \frac{2e \int_0^t E(\tau) d\tau}{\hbar}$..

Now, consider the local BCS states in **Figure 20** put in a loop. If we turn on a magnetic field (say in time T) through the centre of the loop, it will establish a transient electric field in the loop given by

$$\int_0^T E(\tau) = \frac{Ba_r}{2\pi r},$$

where r is radius and a_r the area of the loop. Then, by the above argument, the wavenumber k of the BCS states is shifted by $\Delta k = \frac{(2e) \int_0^T E(\tau)}{\hbar} = \frac{(2e)Ba_r}{2\pi r \hbar}$. Since we have closed loop with $\Phi_0 = Ba_r$

$$\Delta k(2\pi r) = \frac{2e\Phi_0}{\hbar} = 2\pi, \qquad (42)$$

giving

$$\Phi_0 = Ba_r = \frac{h}{2e}.$$

This is the magnetic quantum flux. When one deals with the superconducting loop or a hole in a bulk superconductor, it turns out that the magnetic flux threading such a hole/loop is quantized [9, 10] as just shown.
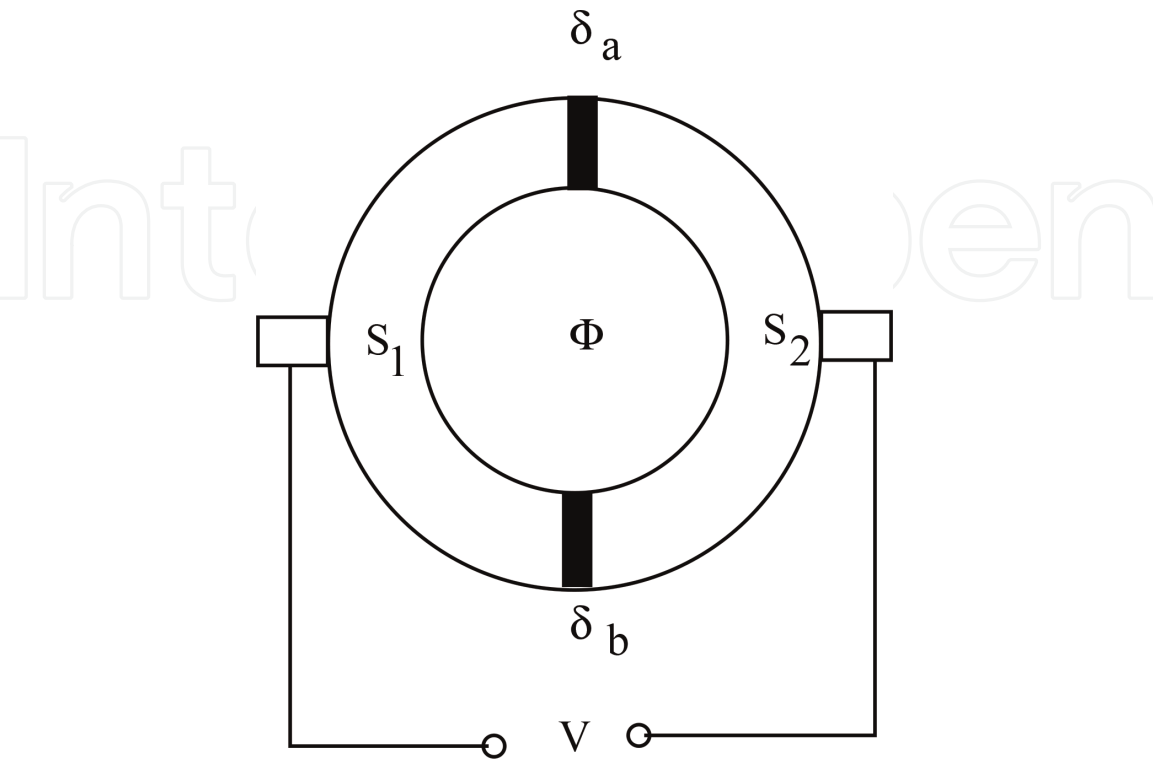

Figure 21.
Depiction of the schematic of a SQUID where two superconductors S$_1$ and S$_2$ are separated by thin insulators.

Figure 21 depicts the schematic of a superconducting quantum interference device (SQUID) where two superconductors S_1 and S_2 are separated by thin insulators. A small flux through the SQUID creates a phase difference in the two superconductors (see discussion on Δk above) leading to the flow of supercurrent. If an initial phase, δ_0 exists between the superconductors. Then, this phase difference after application of flux is from Eq. (42), $\delta_a = \delta_0 + \frac{e\Phi_0}{\hbar}$ across top insulator and $\delta_a = \delta_0 - \frac{e\Phi_0}{\hbar}$ across bottom insulator (see **Figure 21**). This leads to currents $J_a = I_0 \sin \delta_a$ and $J_b = I_0 \sin \delta_b$ through top and down insulators. The total current $J = J_a + J_b = 2I_0 \sin \delta_0 \cos \frac{e\Phi_0}{\hbar}$. This accumulates charge on one side of SQUID and leads to a potential difference between the two superconductors. Therefore, the flux is converted to a voltage difference. The voltage oscillates as the phase difference $\frac{e\Phi_0}{\hbar}$ goes in integral multiples of π for every flux quanta Φ_0. SQUID is the most sensitive magnetic flux sensor currently known. The SQUID can be seen as a flux to voltage converter, and it can generally be used to sense any quantity that can be transduced into a magnetic flux, such as electrical current, voltage, position, etc. The extreme sensitivity of the SQUID is utilized in many different fields of applications, including biomagnetism, materials science, metrology, astronomy and geophysics.

6. Meissner effect

When a superconductor placed in an magnetic field is cooled below its critical T_c, we find it expel all magnetic field from its inside. It does not like magnetic field in its interior. This is shown in **Figure 22**.

German physicists Walther Meissner and Robert Ochsenfeld discovered this phenomenon in 1933 by measuring the magnetic field distribution outside superconducting tin and lead samples. The samples, in the presence of an applied magnetic field, were cooled below their superconducting transition temperature, whereupon the samples canceled nearly all interior magnetic fields. A superconductor with little or no magnetic field within it is said to be in the Meissner state. The Meissner state breaks down when the applied magnetic field is too large. Superconductors can be divided into two classes according to how this breakdown occurs. In type-I superconductor if the magnetic field is above certain threshold H_c, no expulsion takes place. In type-II superconductors, raising the applied field past a critical value H_{c1} leads to a mixed state (also known as the vortex state) in which an increasing amount of magnetic flux penetrates the material, but there remains no
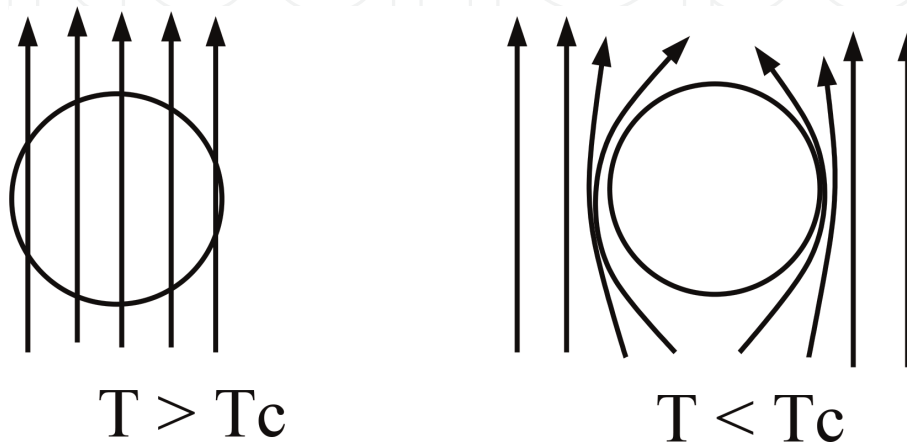

T > Tc   T < Tc

Figure 22.
Depiction of the Meissner effect whereby the magnetic field inside a superconductor is expulsed when we cool it below its superconducting temperature T_c.
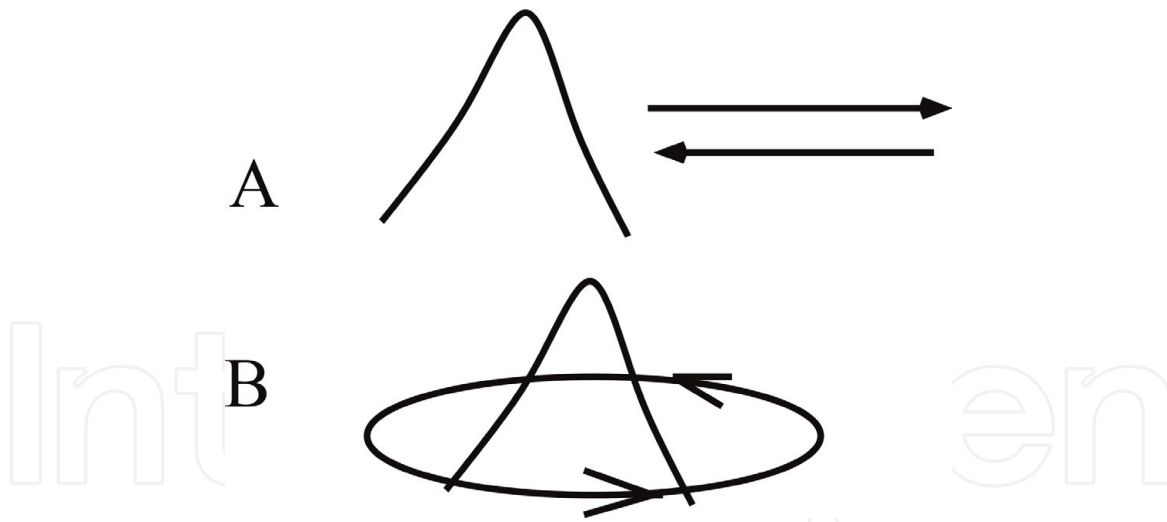
Figure 23.
(A) Depiction on how packets shuttle back and forth in local potential and (B) how they execute a cyclotron motion in the presence of a magnetic field.

resistance to the electric current as long as the current is not too large. At a second critical field strength H_{c2}, no magnetic field expulsion takes place. How can we explain Meissner effect?

We talked about how wave packets shuttle back and forth in local potentials and get bound by phonons to form a BCS molecule. In the presence of a magnetic field, they do not shuttle. Instead, they do cyclotron motion with frequency $\omega = \frac{eB}{m}$. This is shown in **Figure 23**. At a field of about 1 Tesla, this is about 10^{11} rad/s. Recall our packets had a width of $\omega_D \sim 10^{13}$ Hz and the shuttling time of packets was 10^{-13} s, so that the offsets in a packet do not evolve much in the time the packet is back. But, when we are doing cyclotron motion, it takes 10^{-11} s (at 1 T field) to come back, and by that time, the offsets evolve a lot, which means poor binding. It means in the presence of magnetic field we cannot bind well. Therefore, physics wants to get rid of magnetic field, bind and lower the energy. Magnetic field hurts binding and therefore it is expelled. But if the magnetic field is increased, then the cyclotron frequency increases, and at a critical value, our packet returns home much faster, allowing for little offset evolution; therefore, we can bind and there is no need to expulse the magnetic field. This explains the critical field.

7. Giaever tunnelling

When we bring two metals in proximity, separated by a thin-insulating barrier, apply a tiny voltage nd then the current will flow in the circuit. There is a thin-insulating barrier, but electrons will tunnel through the barrier. Now, what will happen if these metals are replaced by a superconductor? These are a set of experiments carried out by Norwegian-American physicist Ivar Giaever who shared the Nobel Prize in Physics in 1973 with Leo Esaki and Brian Josephson "for their discoveries regarding tunnelling phenomena in solids". What he found was that if one of the metals is a superconductor, the electron cannot just come in, as there is an energy barrier of Δ, the superconducting gap. Your applied voltage has to be at least as big as Δ for tunneling to happen. This is depicted in **Figure 24**. Let us see why this is the case.

Recall in our discussion of superconducting state that we had $2p$ pockets of which p were empty. We had a binding energy of $-\frac{4\hbar d^2 N p^2}{\omega_d}$. What will it cost to
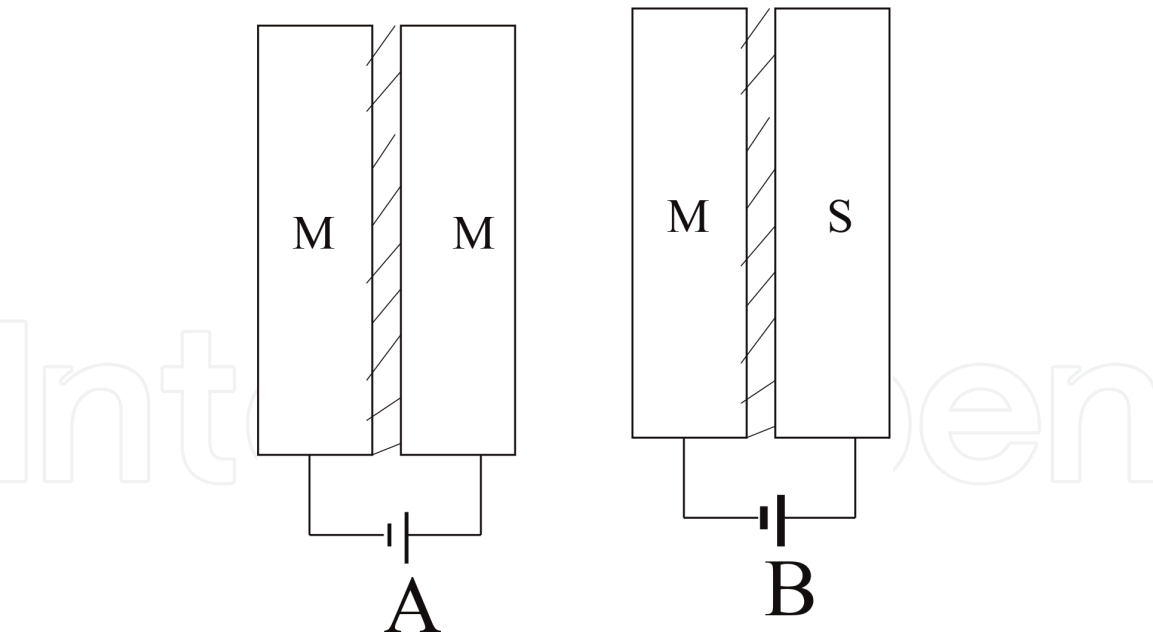
Figure 24.
(A) Depiction on how a tiny voltage between two metals separated by an insulating barrier generates current that goes through an insulating barrier through tunneling. (B) If one of the metals is a superconductor, then the applied voltage has to be at least as big as the superconducting gap.
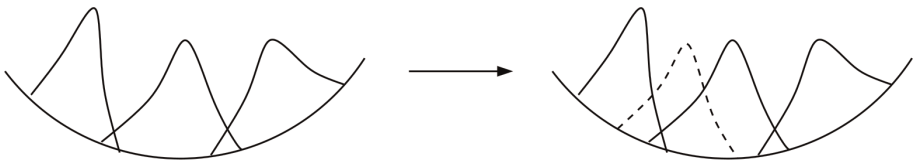

Figure 25.
Depiction on how upon tunneling an extra electron, shown in dashed lines, enters the superconducting state.

bring in an extra electron as shown in **Figure 25**? It will go in one of the empty pockets, and then we have only $p - 1$ pockets left to scatter to reducing the binding energy to $-\frac{4\hbar d^2 N p (p-1)}{\omega_d}$ with a change $\Delta = \frac{4\hbar d^2 N p}{\omega_d}$. Therefore, the new electron raises the energy by Δ, and therefore to offset this increase of energy, we have to apply a voltage as big as Δ for tunneling to happen.

8. High T_c in cuprates

High-temperature superconductors (abbreviated high-T_c or HTS) are materials that behave as superconductors at unusually high temperatures. The first high-T_c superconductor was discovered in 1986 by IBM researchers Georg Bednorz and K. Alex Müller, who were awarded the 1987 Nobel Prize in Physics "for their important break-through in the discovery of superconductivity in ceramic materials".

Whereas "ordinary" or metallic superconductors usually have transition temperatures (temperatures below which they are superconductive) below 30 K (243.2°C) and must be cooled using liquid helium in order to achieve superconductivity, HTS have been observed with transition temperatures as high as 138 K (135°C) and can be cooled to superconductivity using liquid nitrogen. Compounds of copper and oxygen (so-called cuprates) are known to have HTS properties, and the term high-temperature superconductor was used interchangeably with cuprate superconductor. Examples are compounds such as lanthanum strontium copper oxide (LASCO) and neodymium cerium copper oxide (NSCO).

Let us take lanthanum copper oxide La_2CuO_4, where lanthanum donates three electrons and copper donates two and oxygen accepts two electrons and all valence is satisfied. The Cu is in state Cu^{2+} with electrons in d^9 configuration [11]. d orbitals are all degenerated, but due to crystal field splitting, this degeneracy is broken, and $d_{x^2-y^2}$ orbital has the highest energy and gets only one electron (the ninth one) and forms a band of its own. This band is narrow, and hence all k states get filled by only one electron each and form Wannier packets that localize electrons on their respective sites. This way electron repulsion is minimized, and in the limit $U \gg t$ (repulsion term in much larger than hopping), we have Mott insulator and antiferromagnetic phase.

When we hole/electron dope, we remove/add electron to $d_{x^2-y^2}$ band. For example, $La_{2-x}Sr_xCuO_4$ is hole doped as Sr has valence 2 and its presence further removes electrons from copper. $Nd_{2-x}Ce_xCuO_4$ is electron doped as Ce has valence 4 and its presence adds electrons from copper. These extra holes/electrons form packets. When we discussed superconductivity, we discussed packets of width ω_d. In d-bands, a packet of this width has many more k states as d-bands are narrow and only 1–2 eV thick. This means N (k-points in a packet) is very large and we have much larger gap Δ and T_c. This is a way to understand high T_c, d-wave packets with huge bandwidths. This is as shown in **Figure 26**. As we increase doping and add
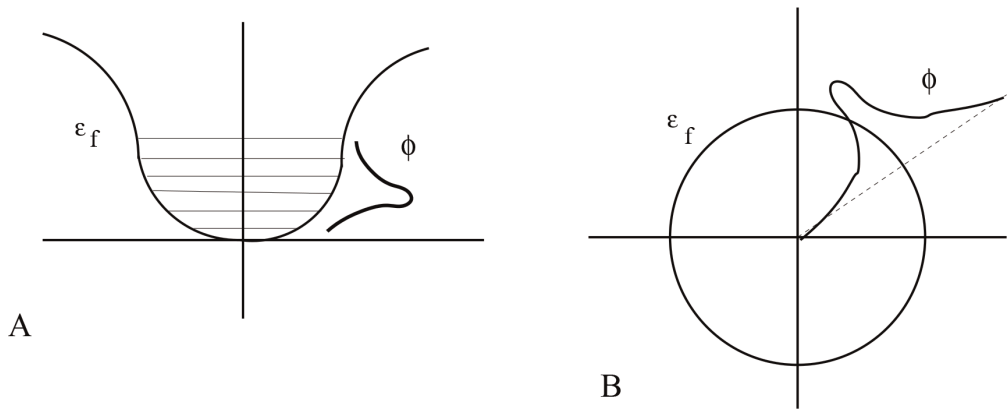

Figure 26.
(A) Depiction on how in narrow d *band the electron wave packet comprises all* k *points to minimize repulsion.*
(B) The wave packet in two dimensions with wave packet formed from superposition of k-points (along the k-direction) inside the Fermi sphere.
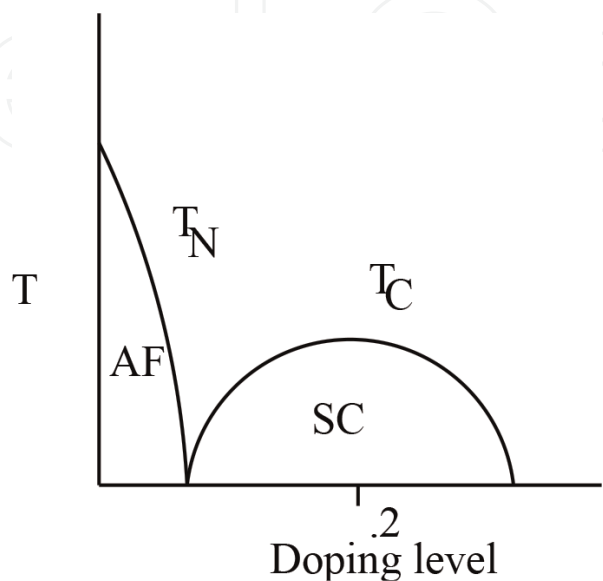

Figure 27.
The characteristic phase diagram of a high T_c *cuprate. Shown are the antiferromagnetic insulator (AF) phase on the left and* dome*-shaped superconducting phase (SC) in the centre.*

more electrons, the packet width further increases till it is $\gg \omega_d$; then, we have significant offset evolution, and binding is hurt leading to loss of superconductivity. This explains the *dome* characteristic of superconducting phase, whereby superconductivity increases and then decreases with doping. The superconducting *dome* is shown in **Figure** 27.

Author details

Navin Khaneja
IIT Bombay, Powai, India

*Address all correspondence to: navinkhaneja@gmail.com

IntechOpen

References

[1] Tinkham M. Introduction to
Superconductivity. 2nd ed. New York,
USA: McGraw Hill; 1996

[2] De Gennes PG. Superconductivity of
Metals and Alloys. New York, USA:
W.A. Benjamin, Inc; 1966

[3] Bardeen J, Cooper L, Schriffer JR.
Theory of superconductivity. Physical
Review. 1957;**108**(5):1175

[4] Kittel C. Introduction to Solid State
Physics. 8th ed. John Wiley and Sons;
2005

[5] Ashcroft NW, Mermin D. On
a new method in the theory of
superconductivity. Solid State Physics.
Harcourt College Publishers; 1976

[6] Simon S. Oxford Solid State Basics.
New Delhi, India: Oxford University
Press; 2013

[7] Kittel C, Kroemer H. Thermal
Physics. Orlando, USA: Freeman and
Co; 2002

[8] Bogoliubov NN. Nuovo Cimento.
1958;7:794

[9] Deaver B, Fairbank W. Experimental
evidence for quantized flux in
superconducting cylinders. Physical
Review Letters. 1961;7(2):43-46

[10] Doll R, Näbauer M. Experimental
proof of magnetic flux quantization in a
superconducting ring. Physical Review
Letters. 1961;7(2):51-52

[11] Khomskii D. Transition Metal
Compounds. Cambridge University
Press; 2014